Ultrasonic Flaw Detection Based on Mathematical Morphology

Jafar Saniie, *Senior Member, IEEE* and Motaz A. Mohamed

***Abstract*—In this paper, the deterministic and statistical properties of morphological filters and their application in ultrasonic flaw detection have studied utilizing different structuring elements. It has been shown the effectiveness of the filtering process depends on the frequency content of input signals, the combination of morphological operations, and the parameters of the structuring elements. The statistical parameters (mean, variance, and skewness) of sequential morphological operations (i.e., dilation, closing, clos-erosion, and clos-opening) are examined in order to determine the noise suppression capability of morphological filters and their biasing effects. Experimental evaluation of morphological filters for flaw detection in the presence of strong scattering echoes is presented for A- and B-scans. The processed experimental results show that morphological filters can improve flaw visibility by suppressing microstructure scattering echoes. The performance of morphological filters is compared with that of recursive median filters and ensemble averaging using experimental data. Results indicate that morphological filters perform better than recursive median filters in preserving the geometric structure of the signal and can replace ensemble averaging which requires numerous measurements.**

I. Introduction

ULTRASONIC flaw detection is an important technique to assure the quality of materials nondestructively. The goal in detection is to isolate the flaw echo from its background noise (e.g., microstructure scattering echoes or instrumentation noise) and to estimate its exact location. The interfering noise often becomes significant to the point that it masks the detection of flaw echoes. Effective techniques for detecting targets in coherent noise are frequency agility and frequency diversity which have been investigated in radar and ultrasound [1]–[4]. In an ultrasonic imaging system, an adaptation of these techniques, referred to a split-spectrum processing coupled with order statistic filtering [5], has proven to be effective in improving the flaw-to-clutter ratio. However, the performance of split-spectrum processing with rank order statistic filters depends on the number of subbands, the correlation between each subband, and the flaw information in each frequency band of the signal [5]. To complement the existing technique, a novel technique for flaw detection based on morphological filters [6]–[9] is presented in this paper. Morphological filters are attractive for their relatively simple computational demands. The computation is made up of addition, subtraction, and logical comparison. It has been shown that these types of operations can be implemented in VLSI for real-time processing [10]. Moreover, morphological filters are based on geometrical concepts and have a desirable syntactical performance.

The theoretical foundations of mathematical morphology and a wide range of its applications were introduced systematically by Matheron [7] and Serra [8]. Many applications of morphological filters are found in biomedical image processing, metallography, geology, remote sensing, and automated industrial inspection. Recently, mathematical morphology has been used for ultrasonic flaw detection, noise suppression, shape representation, skeletonization, and coding [11]–[23].

In mathematical morphology, a signal is viewed as a set in Euclidean space and is operated on by several set-processing morphological operations. The primitives of morphological operations are erosion and dilation. All other morphological operations are sequences combining erosions and dilations. These operations use a structuring element to interact with the signal and extract information. A structuring element is another signal of a somewhat simpler nature than the signal under processing. The structuring element interacts with the signal under study and transforms it into a new signal which is, in some way, more expressive than the original. By varying the structuring element, different types of information can be extracted from the signal.

In this paper, both deterministic and statistical properties of morphological filters are examined. These properties are used to design morphological filters for flaw detection with optimal performance.

II. Basics of Morphological Operations

In general, signals can be represented either by sets (binary) or functions (multilevel). This classification of signals results in a similar classification for morphological filters, i.e., into set processing and function processing filters. A set processing (SP) filter is a transformation of a set (binary signals and binary structuring elements). A function processing (FP) filter (i.e., an extension of SP) is a transformation of a function by a function (multilevel signal and multilevel structuring element). Therefore, set morphological operations are discussed and then extended to multilevel morphological operations.

Set Morphological Operations

There are two fundamental morphological operators: erosion and dilation. Other operations such as opening and closing are

Manuscript received October 21, 1992; revised and accepted August 30, 1993. This work was supported in part by the Electric Power Research Institute under Grant RP2614-75 and by the Office of Naval Research under Grant N00014-92-J1735.

The authors are with the Department of Electrical and Computer Engineering, Illinois Institute of Technology, Chicago, IL 60616.

IEEE Log Number 9213939.

derived operations defined in terms of erosion and dilation. Dilation is the morphological transformation which combines two sets using a vector addition of set elements [22]. If A and B are two binary sets in N-space (E^N), then the dilation of A by B is

$$A \oplus B = c \in E^N | c = a + b \qquad \text{for some } a \in A \text{ and } b \in B. \tag{1}$$

The morphological dual to dilation is erosion. The erosion of A by B is denoted by $A \Theta B$ and is defined as

$$A \Theta B = x \in E^N | x + b \in A \qquad \text{for every } b \in B. \tag{2}$$

In general, both the erosion and dilation operation are not invertible. A derived operation using erosion and dilation is known as an operating which is defined as

$$A \circ B = (A \Theta B) \oplus B. \tag{3}$$

The dual operation to opening is known as closing. The closing is defined as:

$$A \cdot B = (A \oplus B) \Theta B. \tag{4}$$

The goal of any morphological operation is to manage the loss of information through successive transformations. In order to achieve this, we must consider the properties of morphological set operations. Among the many properties associated with the above morphological operators, several are worth mentioning in this review [8].

Increasing: Dilation, erosion, opening and closing operations are increasing. That is, they preserve the order between sets.

Antiextensivity: The opening operation is antiextensive, i.e., the output of the opening operation is always contained in the original signal. As a dual operation of opening, the closing operation is extensive. That is, the output of the closing operation always contains the original signal.

Idempotence: This is an invariance property for iterations of the morphological operators. That is, the output of the operation remains unchanged if we reapply the operation.

Multilevel Morphological Operations

The extension from a set (binary) signal to a function (multilevel) signal has been introduced by Serra [8] and Sternberg [12] using two different but equivalent approaches. The first approach is based on threshold decomposition [8] and the second approach is derived using the concept of umbra and top [12], [22]. In the first approach, the input function can be represented by a collection of sets by thresholding the input at different levels. These sets are operated on by a morphological set transformation, creating a new family of transformed sets. The new sets represent the output function by summing the transformed sets. Note that the threshold decomposition method is limited to the flat structuring element.

In the second approach, the multilevel operations can be defined as algebraic operations using the concepts of the umbra ($U[\ ]$) and top ($T[\ ]$) surface [22]. The multilevel dilation of function f by a multilevel structuring element s is denoted by $f \oplus s$, and is defined by

$$f \oplus s = T[U[f] \oplus U[s]]. \tag{5}$$

From this definition, multilevel dilation can be computed in terms of a maximum operation and a set of addition operations.

$$(f \oplus s)(x) = \max[f(x - z) + s(z)] \qquad \text{for all } z \in S \text{ and } x - z \in F \tag{6}$$

where F and S are the domain of functions f and s, respectively.

The multilevel erosion of a function f by a multilevel structuring element s is denoted by $f \Theta s$, and is defined by

$$f \Theta s = T[U[f] \Theta U[s]]. \tag{7}$$

Using the above definition, the erosion can be evaluated in terms of a minimum operation and a set of subtraction operations.

$$(f \Theta s)(x) = \min[f(x + z) - s(z)] \qquad \text{for all } z \in S \text{ and } x + z \in F. \tag{8}$$

Multilevel opening and closing are defined in an analogous way to opening and closing in binary morphology [(3) and (4)] and have similar properties. The opening operation is used to suppress positive pulses while a closing is used to suppress negative pulses.

A general morphological filter consists of several morphological operations performed in tandem with the same or different structuring elements. It is important to point out that the order of the operations is critical because different results are obtained depending on which operation is done first. Open-closing and clos-opening are two types of morphological filters used for impulsive noise suppression [21], [24]. The open-closing filter consists of opening followed by closing using the same structuring element ($(A \circ B) \cdot B$). The clos-opening filter consists of closing followed by opening ($(A \cdot B) \circ B$). By using these filters we can obtain smoothed versions of the original signal.

III. Statistical Properties of Morphological Filters

In order to properly apply morphological filters to ultrasonic signals, their statistical properties have been examined. In this section, the effect of the width of flat structuring elements on random input signals with independent and identically distributed samples is investigated using Monte Carlo simulation. Monte Carlo simulation describes the statistical characteristics of the processed signal overcoming the complexity that often arises in direct analysis due to statistical dependency of the results at different stages of morphological operations. In particular, we present the output density functions of sequential morphological operation (i.e., dilation, closing, clos-erosion and close-opening) when applied to signals with uniform and Rayleigh distributions. Also, the mean, variance, and skewness are estimated for each of these density functions to present an interpretation of the noise suppression capability of morphological filters and their biasing effects.

To demonstrate the above objectives, computer simulation has been used to process 300 input data sequences, each with a length of $N = 10\,000$ samples. These simulated signals have been applied to a sequence of morphological operations, i.e.,

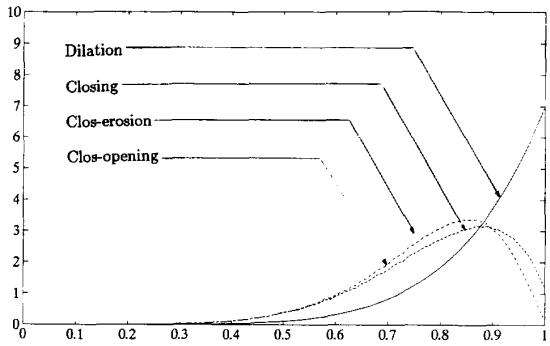

Fig. 1. Probability density functions of dilation, closing, clos-erosion, and clos-opening when the input signal has a uniform density function and using a flat structuring element with a width of 7.

dilation, closing, clos-erosion, and clos-opening using a flat structuring element.

The dilation, closing, clos-erosion, and clos-opening density functions when the samples of the inputs are independent and identically distributed (iid), with uniform density functions (distributed between zero and one) and using a flat structuring element with a width $M = 7$ and height equal to zero are shown in Fig. 1. The mean ($E[\cdot]$), variance ($\sigma^2[\cdot]$) and skewness ($SK[\cdot]$) of the processed density function $p_o(x)$ are estimated in order to investigate the effect of the width (M) of a flat structuring element when input samples have uniform or Rayleigh distributions. The mathematical expressions for these parameters are

$$E[p_o(x)] = \int_{-\infty}^{\infty} x p_o(x)\, dx \tag{9}$$

$$\sigma^2[p_o(x)] = \int_{-\infty}^{\infty} (x - E[p_o(x)])^2 p_o(x)\, dx \tag{10}$$

$$SK[p_o(x)] = \int_{-\infty}^{\infty} (x - E[p_o(x)]^3 p_o(x)\, dx. \tag{11}$$

The mean normalized variance (ratio of output variance over input variance) and skewness are shown in Fig. 2 when the input signals have a uniform density function and flat structuring elements with different widths are used.

These figures indicate that dilation shifts the input signal toward the maximum values and the signal variance is reduced, resulting in a smooth operation. The closing operation (i.e., dilation followed by erosion) is a processing step toward recovering the original signal. Overall, the closing operation tunes down the bias caused by the dilation operation, and slightly increases the signal variance with respect to the dilation operation. The clos-opening operation results in a further smoothing of the signal, where the signal mean and variance are less than those of the closing signal. The mean of dilation, closing, clos-erosion, and clos-opening is shifted to the right (see Fig. 2(a)) due to the effect of dilation as a first operation in the sequence of the above operations. Note that the height of the flat structuring element has no effect on the closing and

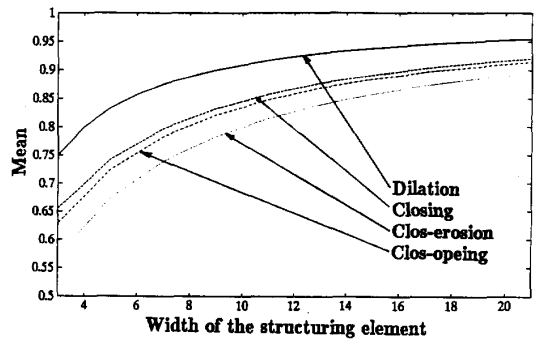

(a)

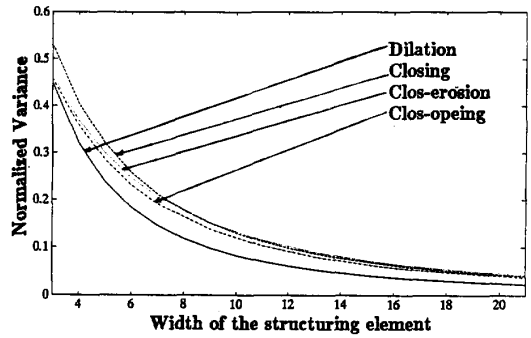

(b)

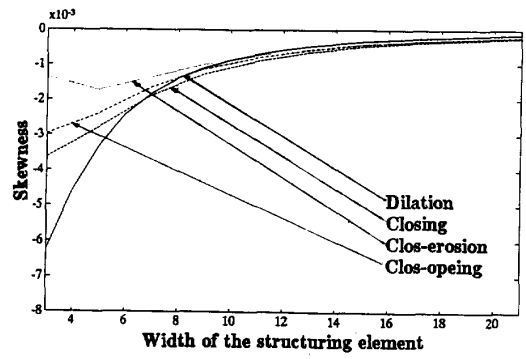

(c)

Fig. 2. Mean normalized variance and skewness of dilation, closing, clos-erosion and clos-opening when the input signal has a uniform density function for a flat structuring element.

clos-opening density function, but shifts the dilation density function to the right and the clos-erosion density function the left by a predictable value depending on the height. In general, the above figures indicate that by increasing the width of the flat structuring element the mean (bias) is increased and the variances of dilation, closing, clos-erosion, and clos-opening output density functions is decreased. Furthermore, dilation has been found to be the most effective step in the smoothing operation. The effect of the other operations following dilation is rather small for larger widths.

The statistical evaluation of morphological operations has been extended for input signals having Rayleigh density func-

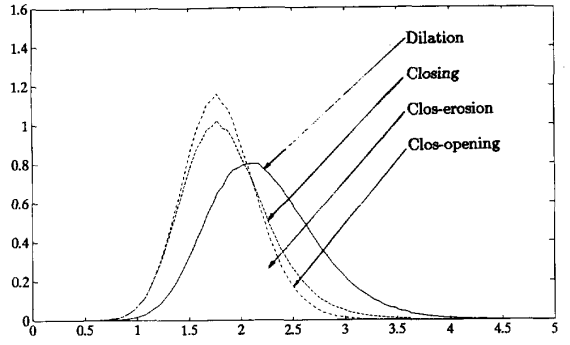

Fig. 3. Probability density functions of dilation, closing, clos-erosion and clos-opening when the input signal has a Rayleigh density function and using a flat structuring element with a width of 7.

tions. Monte Carlo simulation is used to process the data sequence using the same procedure applied to the uniform density function. Fig. 3 shows the effect of a flat structuring element with a width $M = 7$ on dilation, closing, clos-erosion, and clos-opening density function where inputs are iid with a Rayleigh density function ($p(x) = x\exp(-x^2/2), 0 \leq x \leq \infty$). Fig. 4 shows the mean, variance, and skewness of dilation, closing, close-erosion, and clos-opening density functions versus the width of the flat structuring element M for the Rayleigh density function.

Inspection of Figs. 3 and 4 suggests that the overall smoothing capability of the morphological filter applied to an input signal with a Rayleigh density function is similar to the results obtained for input signals with uniform distribution, although some differences can be noted. The dilation density function has the least variance when input signals are uniformly distributed, although the clos-erosion density function has the smallest variance when input signals are Rayleigh distributed. The differences in the variance among dilation, closing, clos-erosion, and clos-opening decrease as the width of the flat structuring element is increased when applied to input signals with a uniform density function. Contrary to this, the differences among dilation, closing, and clos-opening remain significant when the input signals have Rayleigh distributions. Therefore, the results describing the statistics of morphological filters applied to uniform density function can not be used to predict the performance associated with other types of density function.

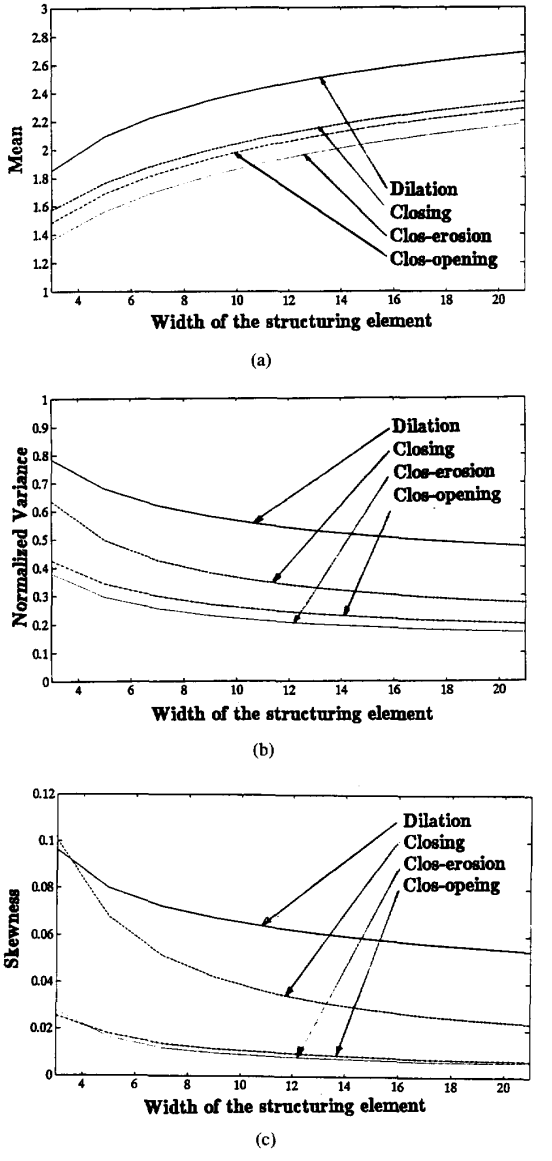

Fig. 4. Mean normalized variance and skewness of dilation, closing, clos-erosion, and clos-opening when the input signal has a Rayleigh density function for a flat structuring element.

IV. Deterministic Properties of Morphological Filters

In order to evaluate the behavior of morphological filters in time domain when applied to ultrasonic signals, the deterministic properties of morphological filters are studied using different structuring elements. In particular, the effect of shape, width and height of structuring elements is examined on the output signal through a sequence of opening and closing operations.

Noise Suppression Using Morphological Operations

In this section, simulation results are presented which illustrate the performance of morphological filters for noise suppression and echo detection. The signal to be processed is a sum of two components: an ultrasonic echo $u(n)$, backscattered from a single reflector and a random noise $v(n)$, i.e.,

$$r(n) = u(n) + v(n) \tag{12}$$

where the ultrasonic echo is assumed to have a Gaussian envelope and is modeled as

$$u(n) = e^{-\alpha n^2}\cos\left(2\pi\frac{f_c}{f_s}n\right). \tag{13}$$

The term f_c is the center frequency, f_s is the sampling rate, and α is a constant related to the bandwidth of the echo and f_s. In this simulation $f_c = 1.25\,\text{MHz}, f_s = 100\,\text{MHz}$ (i.e., the

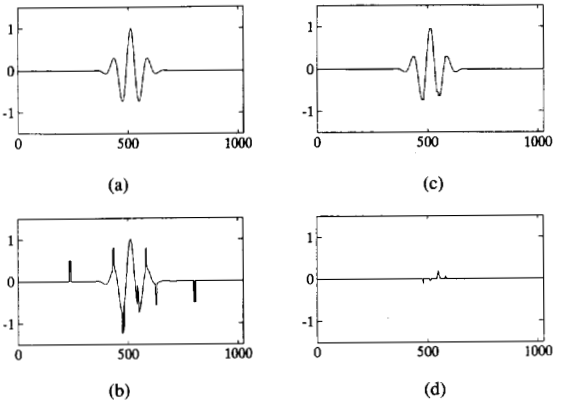

Fig. 5. Impulsive noise suppression using an open-closing operation. (a) Simulated ultrasonic echo. (b) Echo contaminated by random impulsive noise. (c) Recovered signal using open-closing operation. (d) Error signal.

number of samples per cycle of the ultrasonic echo is 80) and $\alpha = 0.0002$.

In ultrasonic measurement, the most common noise is the thermal noise generated in the receiver amplifier. This type of noise is impulsive and has a white spectral density whose level depends on the devices used for amplification. To simulate the thermal noise and evaluate the performance of morphological operators, $v(n)$ is assumed to be random impulsive noise with amplitude of 0.5, and a width of 7 samples. The echo signal, and the echo signal contaminated by impulsive noise is shown in Figs. 5(a) and 5(b), respectively. Fig. 5(b) is processed using an open-closing operation with a flat structuring element (width = 8 samples). Note that the width of the structuring element is larger than the width of impulsive noise and significantly less than the number of samples per cycle of the ultrasonic echo. The opening operation is used to suppress the positive impulses while the closing operation suppresses the negative impulses. Fig. 5(c) and (d) shows the recovered signal and the error (difference) between the actual echo signal and the recovered signal, respectively. These figures show the ability of an open-closing operation for suppressing positive and negative impulsive noise and recovering the original echo signal.

A model of a morphological filter for noise suppression [21] is shown in Fig. 6 which minimizes the bias due to the extensiveness property of opening and closing. In this model, a positively biased estimate of the output signal is obtained by processing the input signal using an open-closing operation. A second negatively biased estimate of the output signal is obtained by processing the input signal using a clos-opening operation. Then a minimum biased output signal is obtained from an average of these two estimates. Fig. 7 presents an example for removing the bias caused by open-closing and clos-opening when applied to an ultrasonic echo. In this simulation f_c = 2.5 MHz and the echo is processed using a half cycle sine structuring element with a height of 0.1 and a width of 23 samples.

To further evaluate the performance of the morphological filter shown in Fig. 6 using different widths of half-cycle sine

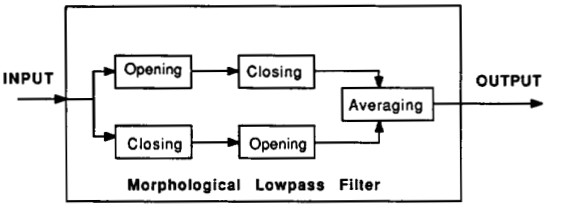

Fig. 6. Block diagram of a low-pass morphological filter for noise suppression.

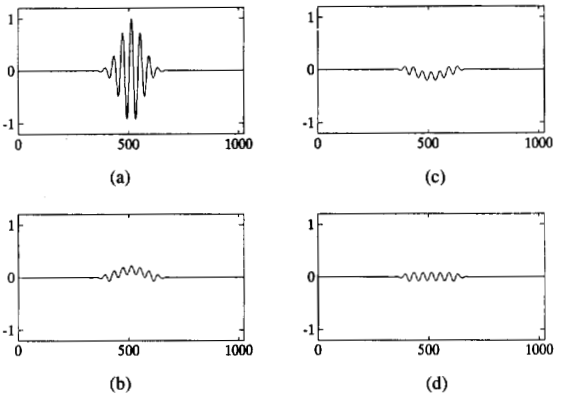

Fig. 7. An example of the output echo at different stages of morphological operations. (a) Input echo. (b) Output of clos-opening. (c) Output of open-closing. (d) Average of open-closing and clos-opening.

structuring element, an ultrasonic echo (Fig. 8(a)) contaminated by impulses uniformly distributed (representing thermal noise) resulting in signal-to-noise of 5.54 dB (see Fig. 8(b)) is processed. Fig. 8(c)–(f) shows the processed results using half-cycle sine structuring elements with different widths (M = 5, 11, 17, and 23 samples) and a height $A = 0.1$. The processed signal shows the effectiveness of the algorithm in suppressing the noise and detecting the ultrasonic echo. Also, the noise suppression is improved by increasing the width of the structuring element. Best signal-to-noise ratio (SNR = 18.65 dB) is obtained when the width of the structuring element is 23 and a height $A = 0.1$.

As a practical application of morphological filters for thermal noise suppression, a typical measured ultrasonic signal with poor SNR (Fig. 9(a)) is processed using the morphological filter (see Fig. 6) and the result is shown in Fig. 9(b). Fig. 9(c) shows the same signal processed using an ensemble averaging of 500 measurements. These results indicate that morphological filters can be used as a replacement for ensemble averaging which requires numerous measurements. In conclusion, the ability of each method to improve the SNR is comparable, although morphological filtering is more efficient.

Filter Classification

In general, various types of morphological filters can be designed using a combination of basic morphological operations with different structuring elements. By varying the structuring element one can extract different types of information from

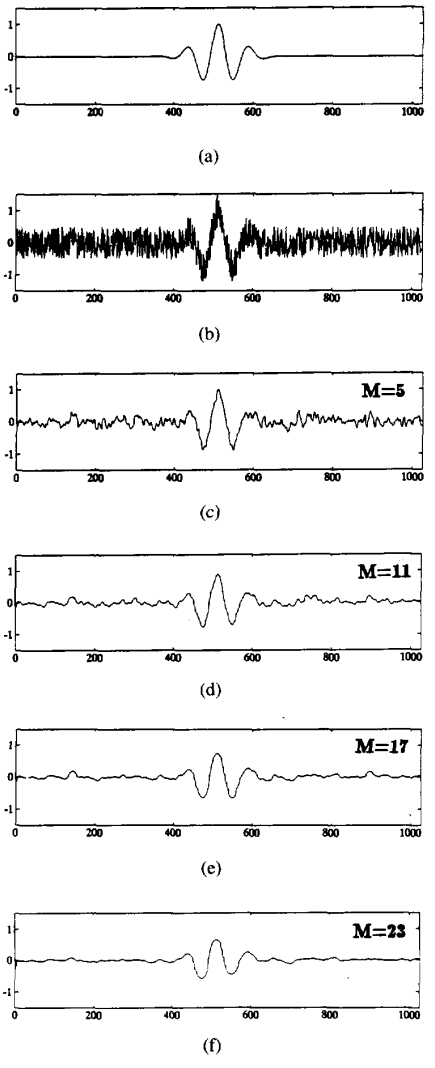

Fig. 8. Noise suppression and echo detection using a low-pass morphological filter.

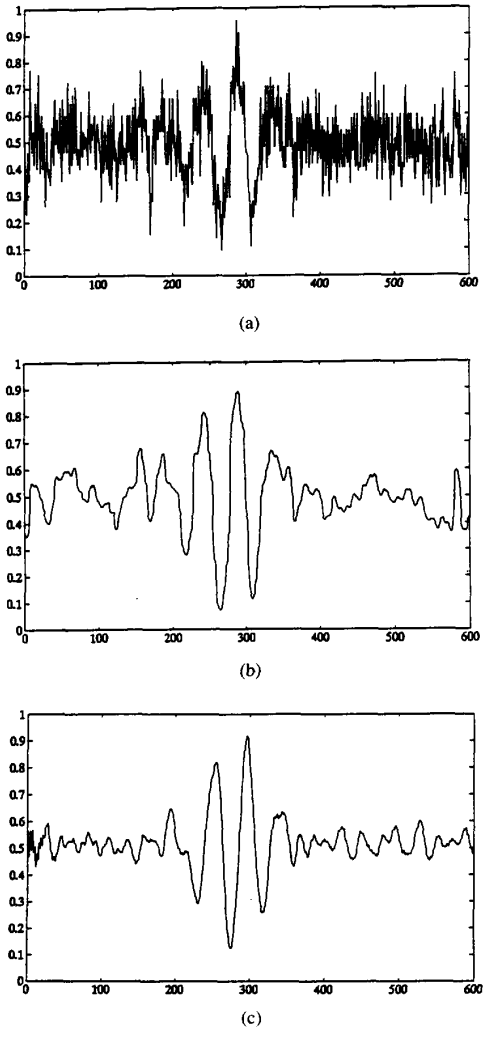

Fig. 9. (a) A typical measured ultrasonic echo with poor signal-to-noise ratio. (b) The processed echo using a low-pass morphological filter. (c) Ensemble average of the echo using 500 measurements.

the signal. In this section, the effect of the parameters of the structuring element on the output signal is examined through a sequence of opening and closing operations. Also, different types of filters are constructed using a sequence of morphological operations in parallel and series.

To demonstrate the effect of the parameters of the structuring elements, the Gaussian envelope echo (13) was used as an input. In this simulation $\alpha = 0.0002$, $f_c = 2.5\,\text{MHz}$, and $f_s = 100\,\text{MHz}$. This signal is processed using the same sequence of morphological operations shown in Fig. 6. Fig. 10(a) shows the processed signal using a flat structuring element with a width M and a constant height equal to zero. The output signal is processed for different values of M. When $M \geq 7$, the output signal begins to attenuate with small distortion until $M = 21$. When $M \geq 21$ the output echo becomes small in value and the echo shape becomes highly distorted. Therefore, using a structuring element with a width less than half the period of the sine function is desirable to preserve the original shape without severe distortion. Fig. 10(b) shows the result of applying the echo to the same morphological operations with a half-cycle sine structuring element. In this case, the output echo is less distorted than the output echo with a flat structuring element of the same width. The half-cycle sine structuring element has a shape similar to the original signal which allows it to penetrate inside the peaks or valleys of the input signal. Therefore, the surface of the output takes the shape of the structuring element.

From the above discussion, it is shown that both the shape and width of the structuring elements affect the output. Height is another factor which affects the output. Fig. 11 shows the effect of the height of a half-cycle sine structuring element when the input signal consists of three echoes with different center frequencies. These echoes are Gaussian envelope cosine functions with frequencies 1.67, 2.5, and 5 MHz (i.e., 60, 40, and 20 samples/cycle). In this simulation f_s = 100 MHz and

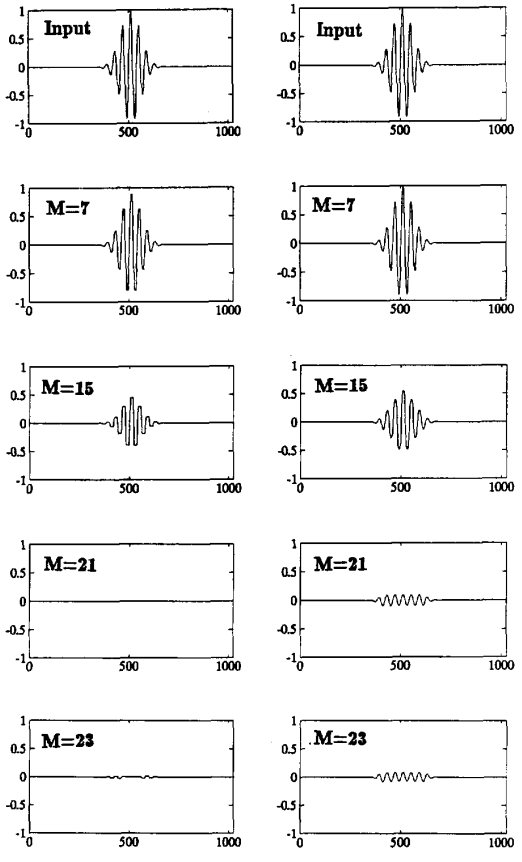

Fig. 10. The effect of the width of a structuring element when applied to an ultrasonic echo for: (a) Flat structuring elements. (b) Half-cycle sine structuring elements.

the width of the structuring element is equal to 11. As the height of the structuring element increases, the output echo becomes more similar to the input echo. The output is almost unaffected by the height when the number of samples/cycle is large compared to the width of the structuring element (60 samples/cycle and width = 11). These results determine when to keep a certain signal feature and discard another.

If an echo with a certain frequency is unmodified, any echoes with a lower frequency will also be unmodified. Furthermore, sequentially alternating the application of opening and closing with the same structuring element removes details of the signal which are small relative to the width of the structuring element. Using linear signal terminology, one can denote these alternating sequential operations as morphological low-pass filters (for example, processing shown in Fig. 6). Morphological high- and band-pass filters can also be designed using morphological low-pass filters with different cutoff frequencies. In summary, recommended designs of low-, high-, and band-pass filter are:

- The low-pass filter is defined as the average of open-closing and clos-opening.

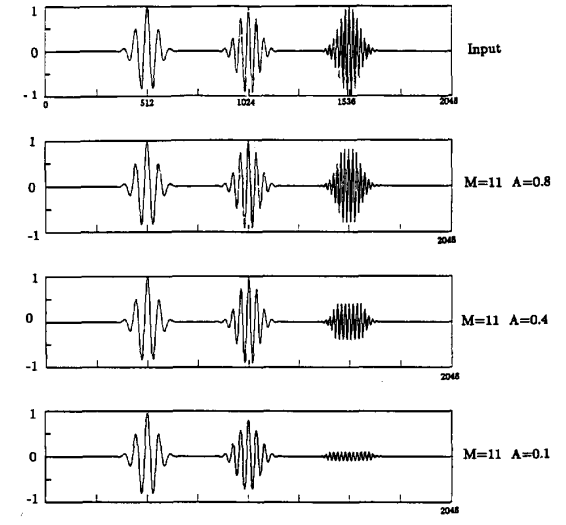

Fig. 11. The effect of height when a half-cycle sine structuring element is used.

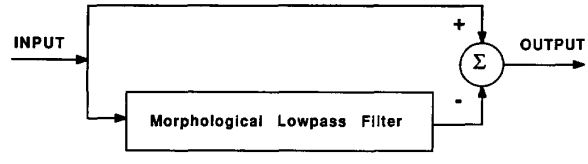

Fig. 12. Block diagram of the high-pass morphological filter.

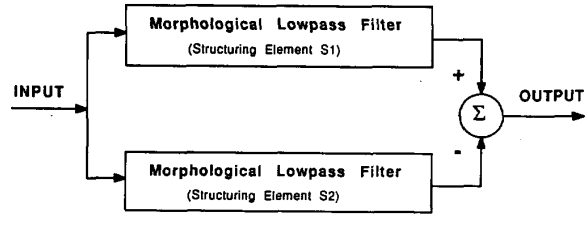

Fig. 13. Block diagram of the band-pass morphological filter.

- The high-pass filter is defined as the original signal minus the average of open-closing and clos-opening.
- The band-pass filter is defined as the difference of two averages of open-closing and clos-opening with two different structuring elements.

The block diagrams of the low-, high-, and band-pass filters are shown in Figs. 6, 12, and 13, respectively. Also, examples of low-, high-, and band-pass filters using half-cycle sine structuring elements are shown in Fig. 14. In Fig. 14(b) and (c), the structuring elements have the same width ($M = 11$) and heights of 0.01 and 0.35, respectively. In Fig. 14(d) the structuring element s_1 has a width of 11 and a height of 0.1 and s_2 has a width of 21 and a height of 0.2. These figures indicate that the parameters of the structuring element and type of morphological operations determine what frequencies of the signal are affected by the filtering process.

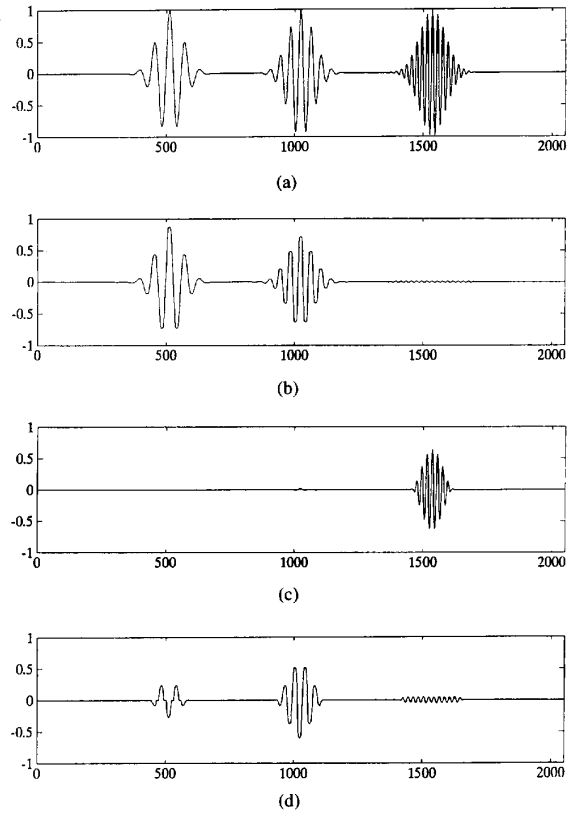

Fig. 14. Examples of low-, high-, and band-pass morphological filter outputs. (a) Input. (b) Low-pass morphological filter. (c) High-pass morphological filters. (d) Band-pass morphological filter.

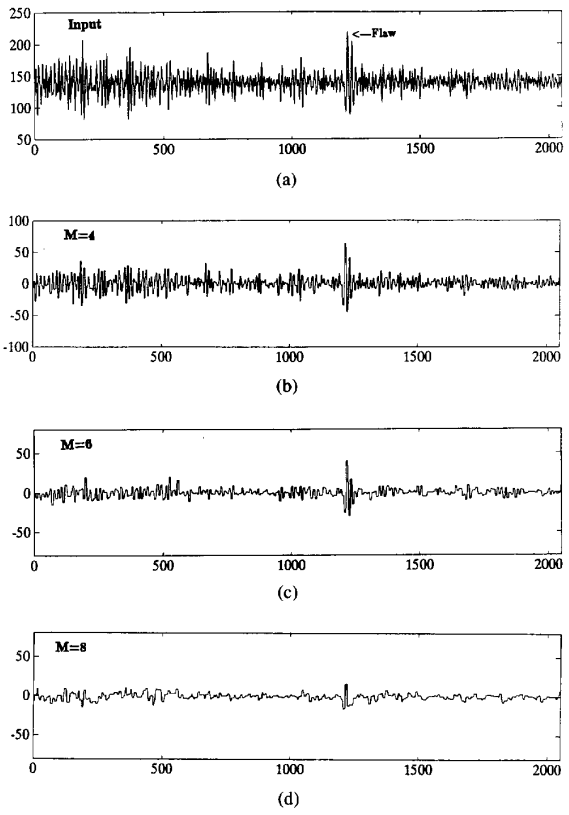

Fig. 15. Flaw echo detection and clutter suppression using low-pass morphological filters with flat structuring elements of different widths (M). (a) is the original measured signal.

It is important to mention that the filtering characteristics of a morphological processor cannot be generalized in terms of frequency response due to nonlinearity. Furthermore, the superposition principle does not apply to these nonlinear filters and defining the filter bandwidth is a meaningless quantity. This study only indicates that the filtering process depends on the frequency content of the input signal as well as the parameters of structuring elements.

V. Morphological Filters for Ultrasonic Flaw Detection

An important application of the morphological filter is in ultrasonic flaw detection when the flaw echo has been contaminated by the microstructure scattering echoes. The goal in detection is to isolate the flaw echo from its background clutter (e.g., microstructure scattering echoes) and to estimate its exact location. The information content of ultrasonic signals has been used to design a suitable structuring element to enhance flaw-to-clutter ratio (FCR). Also, the performance of morphological filters is compared with the performance of recursive median filters to display their similarities.

Experimental Results for Improved Flaw Detection

To illustrate the effectiveness of the parameters of the structuring element in ultrasonic flaw detection, a broadband transducer was used to detect a simulated flaw embedded within a steel block with strong grain scattering. The measurement was achieved using the contact technique and data was acquired with a 100 MHz sampling frequency. A measured A-Scan is shown in Fig. 15(a). This signal was processed by the same sequence of opening and closing operations discussed in the previous section (see Fig. 6). Processed results are shown in Fig. 15(b)–(d) for a flat structuring element with different widths (M = 4, 6, and 8 samples). These results indicate that morphological filters are capable of detecting targets while suppressing clutter.

In order to achieve an optimal performance of morphological filters for clutter suppression and flaw detection, the effect of the width of the flat structuring element in detecting ultrasonic signals was examined using the FCR of the output signal. The FCR of the output signal as a function of the width of a flat structuring element is shown in Fig. 16. This figure shows that the FCR increases as the width approaches the optimal value (M_{op} = 6). The FCR of the output signal at M_{op} = 6 is 1.6 times better than the FCR of the input signal.

To achieve a better design of morphological filters, the number of zero crossings of the processed output signal has been evaluated as a function of the width of the flat structuring element. The calculation results indicate that the number of zero crossings decreases when the width of a flat structuring

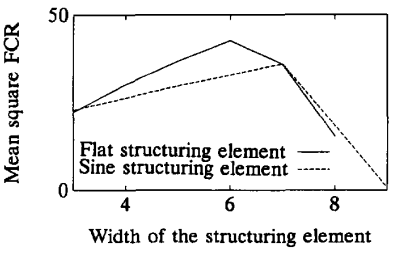

Fig. 16. Flaw-to-clutter ratio of the output signal as a function of the width using: ——— Flat structuring element and – – – half-cycle sine structuring element with a height of 2.0.

element is increased. This simply implies that the smoothing process becomes more effective when the structuring element is wider, although excessive smoothing may eliminate flaw echoes. Therefore, an evaluation of a zero crossing of the A-Scan can lead to an estimation of the optimal width of the structuring element. Since microstructure echoes represent the dominating information, properly removing them requires a structuring element with a width larger than the average duration of the zero crossing of the measured signal. The average width estimated with a zero crossing for the measured signal is 5.14 which is very close to the optimal width M_{op} = 6 of the flat structuring element.

The strength of morphological filters lies in their natural coupling between the shape of the signal and the structuring element. A comparison between the performance of a flat and a half-cycle sine structuring element indicates that the sinusoidal structuring element preserves the original shape of the signal better than the flat structuring element because the surface of the processed signal takes the shape of the structuring element (for clarification, see Fig. 10). However, the flat structuring element smoothes the signal more effectively than the sinusoidal structuring element of the same width. A comparison of the FCR between the flat and sinusoidal structuring elements of the processed signal is shown in Fig. 16. This figure shows that the FCR increases as the width approaches the optimal value (M_{op} = 6 for a flat structuring element, and M_{op} = 7 for a sinusoidal structuring element). In general, these results indicate that a flat structuring element offers better FCR while a sinusoidal structuring element has better syntactical performance in preserving the details of the original signal.

To further improve the resolution and FCR for flaw detection, it is effective to estimate the background echoes (clutter) and then subtract this estimate from the preprocessed signal. This technique can be represented as

$$\hat{y} = y - [(y_o s_2) \cdot s_2 + (y \cdot s_2)_o s_2]/2 \tag{14}$$

where

$$y = [x_o s_1) \cdot s_1 + x \cdot s_1)_o s_1]/2 \tag{15}$$

x is the input signal, s_1 and s_2 are flat structuring elements with lengths of 8 and 10, respectively. It is important to point out that (15) reduces the high-frequency information associated with microstructure scattering (i.e., low-pass filtering). However, the high-pass filtering (i.e., clutter subtraction)

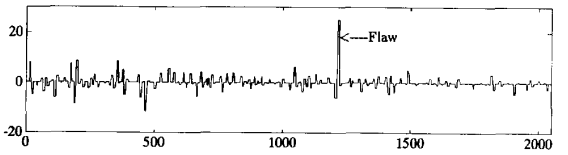

Fig. 17. Processed backscattered flaw signal using a pseudo-band-pass morphological filter.

of this result [(14)] reemphasizes higher frequencies and broadens the bandwidth of the flaw echo. The above morphological processing (combination of (14) and (15)) shows a pseudoband-pass filter response. The processed experimental result using the pseudo-band-pass filter is shown if Fig. 17. This result shows that the background noise is tremendously reduced (FCR is improved by 5.66 dB) while the detection resolution is enhanced.

Comparison of Morphological and Median Filters

A connection between median filters and morphological operations with flat structuring elements was made by Maragos [18], [19]. In particular, a signal is a median root if it is the root of both the opening and closing. Furthermore, medians and their iterations are bounded below by the opening and above by closing, while the median root is bounded below by the open-closing and above by clos-opening. Median filtering [25] is an effective technique for noise suppression (its response is governed by the window size, and it displays low-pass filtering effect). An extension of the median filter is the recursive median filter which results in the output being the median of the last N outputs and the last $N + 1$ inputs. If $\{x(\cdot)\}$ and $\{y(\cdot)\}$ are the input and output of a recursive median filter with window size $M = 2N + 1$, then $y(\cdot)$ is given by

$$y(m) = \text{med}[y(m-n), \cdots, y(m-1), x(m), x(m+1), \cdots, x(m+N)]. \tag{16}$$

It is important to point out that the recursive operation generates a root with only a single pass through the data, where a root is an invariant signal to the filter.

The performance of recursive median filters with different widths (M = 5, 11, and 15 samples) when applied to the same input ultrasonic signal (see Fig. 15(a)) is shown in Fig. 18. This figure shows that the recursive median filter can detect flaw echoes and suppress backscattered noise similar to morphological filters. Note that morphological filters have better syntactical performance in preserving the details of the signal when compared to recursive median filters since they have a flexibility in changing the shape of their structuring elements to match a particular pattern of the original signal.

Morphological Processing of Ultrasonic B-Scans

In this paper, the evaluation of morphological filtering has been extended from A-Scans to B-Scans. A B-Scan experimental measurement is shown in Fig. 19(a). A 5 MHz broadband transducer was used to test a flat bottom hole (0.067") embedded within a steel block as a simulated flaw. This image is processed using the morphological filter shown

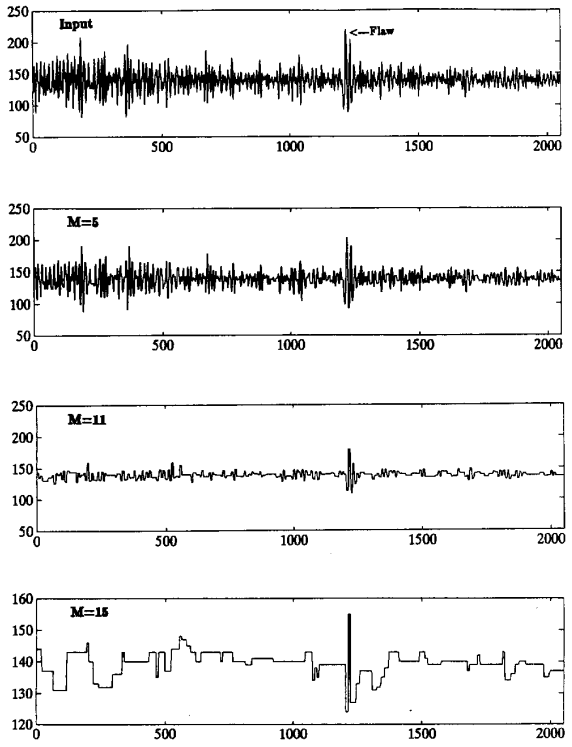

Fig. 18. Flaw echo detection and clutter suppression using recursive median filters with different widths.

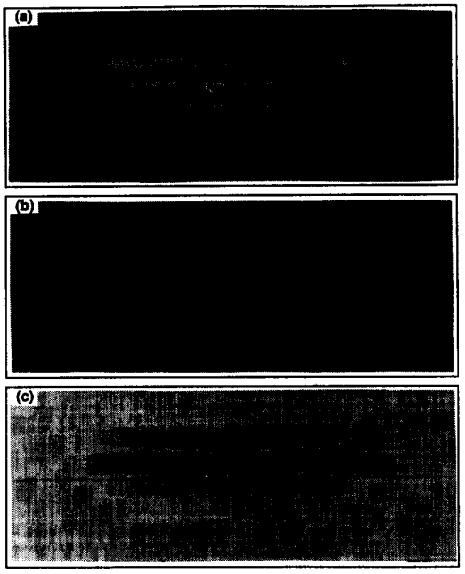

Fig. 19. (a) An experimental B-Scan image of a flat bottom hole in a steel block. (b) The processed B-Scan image using a low-pass morphological filter. (c) The processed B-Scan image using a pseudo-band-pass morphological filter.

in Fig. 6 (low-passing filtering) with a flat structuring element. The zero crossing of the image has been used to design a suitable flat structuring element with an optimal performance. The average duration of the zero crossing of the B-Scan image is 8.08. Therefore, the flat structuring element with a width of 9 samples was chosen for noise removal. The result of the processed image is shown in Fig. 19(b) indicating that the morphological low-pass filter reduces clutter and improves resolution. Further improvement in detection resolution is obtained using the pseudo-band-pass morphological filter [see (14) and (15)]. Flat structuring elements (s_1 and s_2) with lengths 9 and 13, respectively, are used for noise removal. The processed image shown in Fig. 19(c) indicates that the pseudo-band-pass morphological filter improves the ultrasonic B-Scan by reducing the background clutter.

VI. Conclusion

This paper has dealt with the properties of morphological filters and their applications for improving the flaw-to-clutter ratio of ultrasonic signals (A- or B-Scan). Our study has focused on the deterministic and stochastic properties of morphological filters using different structuring elements. Structuring elements are characterized by their width and shape. From both a deterministic and a stochastic point of view, it has been shown that the effectiveness of the filtering process depends on the frequency content of input signals as well as the parameters of the structuring elements. The statistical properties of sequential morphological operations (i.e., dilation, closing, clos-erosion, and clos-opening) have been examined using flat structuring elements applied to signals with uniform and Rayleigh density functions. The simulated results indicate that by increasing the width of the flat structuring element the mean (bias) is increased and the variance and skewness of dilation, closing, clos-erosion, and clos-opening density functions are decreased.

Morphological filters have been applied to detect flaw echoes in ultrasonic signals contaminated by thermal noise or grain scattering noise. The processed experimental results show that morphological filters can detect flaw echoes while suppressing noise. Moreover, it has been shown that morphological filters can replace ensemble averaging which requires numerous measurements. In this study, recursive median filtering has been introduced as an effective method for enhancing the FCR of ultrasonic signals. Recursive median filters, similar to morphological low-pass filters, reduce clutter, and improve flaw detection. However, morphological filters have better performance because of their flexibility in changing the shape of the structuring elements to preserve certain patterns of the original signal.

References

[1] P. F. Guarguaglini, "A unified analysis of diversity radar systems," *IEEE Trans. Aerospace Electronic Sys.*, vol. 4, pp. 418–420, Mar. 1968.
[2] N. M. Bilgutay and J. Saniie, "The effect of grain size on flaw visibility enhancement using split-spectrum processing," *Materials Evaluation*, vol. 42, pp. 808–814, May 1984.
[3] E. W. Beasley and H. R. Ward, "Quantitative analysis of sea clutter decorrelation with frequency agility," *IEEE Trans. Aerospace and Electronic Syst.*, vol. 4, no. 3, pp. 468–473, May 1968.
[4] V. L. Newhouse, N. M. Bilgutay, J. Saniie, and E. S. Furgason, "Flaw-to-grain echo enhancement by split-spectrum processing," *Ultrasonics*, pp. 59–68, Mar. 1982.

[5] J. Saniie, D. T. Nagle, and K. D. Donohue, "Analysis of order statistics filters applied to ultrasonic flaw detection using split spectrum processing," *IEEE Trans. Ultrasonics, Ferroelectrics Frequency Cont.*, vol. 38, pp. 133–140, Mar. 1991.
[6] C. R. Giardina and E. R. Dougherty, *Morphological Methods in Image and Signal Processing*. Englewood Cliffs, NJ: Prentice-Hall, 1988.
[7] G. Matheron, *Random Sets and Integral Geometry*. New York: Wiley, 1975.
[8] J. Serra, *Image Analysis and Mathematical Morphology*. New York: Academic, 1982.
[9] I. Pitas and A. N. Venetsanopoulos, *Nonlinear Digital Filters: Principles and Applications*. Kluwer Academic, 1990.
[10] E. J. Coyle, "The theory and VLSI implementation of stack filters," *VLSI Signal Processing II*. New York: IEEE Press, 1986, pp. 141–151.
[11] M. A. Mohamed and J. Saniie "Application of morphological filters in ultrasonic flaw detection," *IEEE Ultrasonic Sympo. Proc.*, pp. 1157–1161, 1990.
[12] S. R. Sternberg, "Gray scale morphology," *Comp. Vision, Graphics, Image Process.*, vol. 35, no. 3, pp. 333–355, 1986.
[13] I. Pitas and A. N. Venetsanopoulos, "Morphological shape decomposition," *Pattern Anal. Machine Intell.*, vol. PAMI-12, no. 1, pp. 38–45, Jan. 1990.
[14] P. A. Maragos and R. W. Schafer, "Morphological skeleton representation and coding of binary image," *IEEE Trans. Acoust., Speech, Signal Processing*, vol. 34, pp. 1228–1244, Oct. 1986.
[15] P. Maragos, "Tutorial on advances in morphological image processing and analysis," *Optical Eng.*, vol. 26, pp. 623–632, July 1987.
[16] V. Goetcherian, "From binary to gray tone image processing using fuzzy logic concepts," *Pattern Recognition*, vol. 12, pp. 7–15, 1980.
[17] R. Crimmins and W. M. Brown "Image algebra and automatic shape recognition," *IEEE Trans. Aerospace Electronic Syst.*, vol. 21, no. 1, pp. 60–69, 1985.
[18] P. A. Maragos and R. W. Schafer, "Morphological filters—Part I: Their set-theoretic analysis and relations to linear shift-invariant filters," *IEEE Trans. Acoust., Speech, Signal Process.*, vol. 35, pp. 1153–1169, Aug. 1987.
[19] ——, "Morphological filters—Part II: Their set-theoretic analysis and relations to linear shift-invariant filters," *IEEE Trans. Acoust., Speech, Signal Process.*, vol. 35, pp. 1170–1184, Aug. 1987.
[20] C. H. G. Wright, E. J. Delp, and N. C. Gallagher, "Nonlinear target enhancement for the hostile nuclear environment," *IEEE Trans. Aerospace Electronic Syst.*, vol. 26, no. 1, pp. 122–145, Jan. 1990.
[21] C. H. Chu and E. J. Delp, "Impulsive noise suppression and background normalization of electrocardiogram signals using morphological operators," *IEEE Trans. Biomed. Eng.*, vol. 36, pp. 262–273, Feb. 1989.
[22] R. M. Haralick, S. R. Sternberg, and X. Zhuang, "Image analysis using mathematical morphology," *IEEE Trans. Pattern Anal. Mach. Intell.*, vol. 9, pp. 532–550, July 1987.
[23] J. Song, R. Stevenson, and E. J. Delp, "The use of mathematical morphology in image enhancement," in *Proc. 32nd Midwest Symp. Circ. Sys.*, pp. 67–70, Aug. 1989.
[24] R. L. Stevenson and G. R. Arce, "Morphological filters: Statistics and further syntactic properties," *IEEE Trans. Circ. Syst.*, vol. 34, no. 11, pp. 1292–1305, Nov. 1987.
[25] N. C. Gallagher, J. and G. L. Wise, "A theoretical analysis of median filters," *IEEE Trans. Acoust., Speech, Signal Process.*, vol. 29, pp. 1136–1141, Dec. 1981.

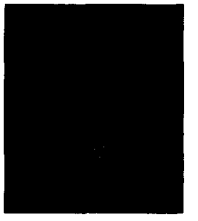

Jafar Saniie (SM'91) was born in Iran on March 21, 1952. He received the B.S. degree in electrical engineering from the University of Maryland in 1974. He received the M.S. degree in biomedical engineering in 1977 from Case Western Reserve University, OH, and the Ph.D. degree in electrical engineering from Purdue University, IN.

In 1981, he joined the Department of Applied Physics, University of Helsinki, Finland, to conduct research in photothermal and photoacoustic imaging. Since 1983, he has been with the Department of Electrical and Computer Engineering at Illinois Institute of Technology where he is a Professor and Director of the Ultrasonic Information Processing Laboratory. His current research activities include radar signal processing, estimation and detection, ultrasonic imaging, nondestructive testing and digital hardware design.

Dr. Saniie is a Technical Committee member of the *IEEE Ultrasonics Symposium*, Program Coordinator of the *Conference on Properties and Applications of Magnetic Materials*, and Editorial Advisory member of the *Nondestructive Testing and Evaluation Journal*. He is a member of Sigma Xi, IEEE, Tau Beta Pi, Eta Kappa Nu, and has been IEEE Branch Counselor (1983–1990). He is the 1986 recipient of the Outstanding IEEE Student Counselor Award.

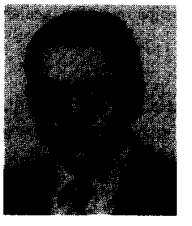

Motaz A. Mohamed was born in Assiut, Egypt on February 3, 1956. He received the B.S. and M.S. degrees in electrical engineering from Assiut University, Egypt, in 1978 and 1983. In 1992, he received the Ph.D. degree in electrical and computer engineering from Illinois Institute of Technology, Chicago, Ill. His Ph.D. work was supported by the Peace Fellowship sponsored by the Egyptian Government.

From 1983 to 1987, he was an Assistant Lecturer in the Electrical Engineering Department, Assiut University. Presently, Dr. Mohamed is an Assistant Professor in the Electrical Engineering Department, Assiut University. His research interests are in nonlinear signal processing, statistical analysis, and ultrasonic imaging.